CRREL REPORT 90-11

# UHF Model Simulation of Detecting Voids in a Dielectric Medium Using HF-VHF Airborne Short-Pulse Radar

Steven A. Arcone

December 1990

*For conversion of SI metric units to U.S./British customary units of measurement consult ASTM Standard E380,* Metric Practice Guide, *published by the American Society for Testing and Materials, 1916 Race St., Philadelphia, Pa. 19103.*

*Cover: Radar profiling of scale model tunnels in sand.*

CRREL Report 90-11

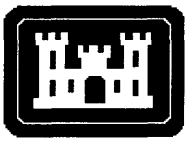

**U.S. Army Corps of Engineers**
Cold Regions Research & Engineering Laboratory

# UHF Model Simulation of Detecting Voids in a Dielectric Medium Using HF-VHF Airborne Short-Pulse Radar

Steven A. Arcone

December 1990

Prepared for
U.S. ARMY BELVOIR RD&E CENTER

## PREFACE

This report was prepared by Dr. Steven A. Arcone, Geophysicist, Snow and Ice Branch, Research Division, U.S. Army Cold Regions Research and Engineering Laboratory. The work reported here was supported by the U.S. Army Belvoir RD&E Center, Ft. Belvoir, Virginia, under Task No. A0H20010181.

Technical review of this report was provided by M. Moran and D. Albert, both of CRREL.

## CONTENTS



## ILLUSTRATIONS

Figure

# UHF Model Simulation of Detecting Voids in a Dielectric Medium Using HF-VHF Airborne Short-pulse Radar

STEVEN A. ARCONE

## INTRODUCTION

Underground void detection has received considerable attention in the last 20 to 25 years. Of the several geophysical detection methods available (e.g., electromagnetic induction, short-pulse radar, seismic, cross-borehole tomography), short-pulse radar offers the unique combination of having the highest resolution and the highest rate of data acquisition, and being usable from an aircraft for targets within about 50 m of the surface. Short-pulse radar has been used most often for near-surface studies of soils (e.g., Annan and Davis 1976, Shih and Doolittle 1987), groundwater (e.g., Delaney et al. 1990) and ice (e.g., Kovacs and Morey 1985, Arcone and Delaney 1987) at pulse center frequencies between 100 and 500 MHz, a frequency range for which antennas are readily available commercially. Frequencies below 100 MHz provide greater penetration, but have been used mainly in low loss media such as glaciers (e.g., Watts and England 1976, Watts and Wright 1981, Jacobel and Anderson 1987) and permafrost (e.g., Dallimore and Davis 1987). Short-pulse radar, and also cross-borehole, one-way transmission techniques, have been used for surface-based studies of crevasses, voids, conduits and mine drifts in glaciers (Jezek et al. 1979, Jacobel and Anderson 1987), bedrock and sediments (e.g., Moffatt and Puskar 1976, Annan et al. 1988, Greenfield 1988, Moran 1989), and pavement (e.g., Steinway et al. 1981). This paper discusses the results of a scale model operating in the UHF (ultra-high frequency: 300–3000 MHz) band to study the use of frequencies below 100 MHz in the HF (3–30 MHz) to VHF (30–300 MHz) bands for an airborne survey to detect voids in a dielectric medium of low conductivity, such as crystalline bedrock or ice. The airborne mode is chosen for its high rate of ground coverage.

Airborne subsurface radar surveys have been applied most successfully to depths less than 5 m, using antennas radiating waveforms with center frequencies of 500 MHz and above (e.g., Arcone and Delaney 1987, Delaney et al. 1990). These frequencies use small antennas that are shielded to reduce clutter (extraneous, unwanted reflections), especially from the aircraft. Frequencies less than 100 MHz are required for deeper penetration because they limit conductive attenuation and surface and volume scattering losses. Such frequencies require meter-sized transmit and receive antennas separated by several meters, a cumbersome arrangement for airborne or surface surveys. Short-pulse antennas are usually linear in the 10- to 50-MHz range and unshielded to reduce size and weight (e.g., Watts and Wright 1981). Polarization parallel to the survey direction is thus preferable because the transmit and receive antennas can be towed in parallel or co-linearly, which makes the configuration easier to tow both in air and on the ground surface. Unshielded antennas have worked well at high altitudes (Watts and Wright 1981), but at very low altitudes have been subject to severe clutter between the aircraft and ground surface (Arcone 1988). Thus, antenna shielding may be necessary to avoid this clutter as well as to avoid distortion of the transmitted pulse by the aircraft structure. Shielded antennas were used in this study because it is the intention of this research to develop such antennas operating at less than 100 MHz.

Theoretically, dielectric cylinders show rapid fluctuations in backscattered signal strength as the radius-to-wavelength ratio varies, especially for electric field polarization perpendicular to the strike of the void axis, as suggested by data discussed in Ruck et al. (1970). These fluctuations are attributable to internal and surface resonances, which could distort the reflected waveforms as they continually leak radiation. Moran (1989)

and Greenfield (1988) have shown that some distortion of the forward scattered waveform can occur for polarization perpendicular to the strike of the void axis. Jacobel and Anderson (1987), using pulse center frequencies down to 4 MHz, document short-pulse radar distortion from water bodies within glaciers. They use the waveforms to calculate an approximate lower limit on the void dimensions. Arcone (1990) has reported void resonances in the data in this paper, but further filtering discussed later will show this not to be the case.

The objective of this study was to determine by modeling the response of a square cross-sectional void embedded in a dielectric medium to an airborne-launched pulse that was polarized both parallel and transverse to the direction of the void axis. The model frequency was chosen to give an in-situ wavelength comparable to the void sizes in anticipation that this would give a good combination of strong response and good penetration at full scale. If a significant interaction was found, the research would then proceed to construct HF–VHF band transducers for field study, and eventually adapt them for airborne work.

The modeling scales were 10, 20 and 40:1 for a void size of 2 m. A 2.5- × 4.5-m rectangular concrete box, 1-m deep, was filled with sand having a measured bulk dielectric constant of about 5.9, which is in the range of many types of crystalline bedrock. Embedded in the sand were three square Styrofoam (dielectric constant less than 1.1) strips having side lengths of 5, 10 and 20 cm. Airborne radar profiles were run across the box using antennas, mounted on a boom off a tractor, that radiated nanosecond pulses at a center frequency near 870 MHz. This frequency thus allowed modeling the response of a 22-, 44- and 87-MHz short-pulse wavelet to a 2-m size void. Polarizations both perpendicular and parallel to the void axes were used.

## RADAR SYSTEM

Commercially available short-pulse radar (also known as impulse, subsurface or ground-penetrating radar) consists of a control unit, antennas and cables, magnetic tape recorder and a power supply. The control unit generates timing signals to key the transmitter on and off and synchronizes this keying with the receiver. It controls the scan rate (how fast individual echo scans are compiled), the time range over which one wants to view the echoes, and the gain to be applied to the echoes. The antennas are usually separated (transmit and receive) and are designed to radiate and receive a broadband pulse of only a few to tens of nanoseconds duration. Consequently, the antennas have very little gain. Electronics for the transmitter and receiver are usually incorporated into the antenna housing. The VHF–UHF received signals are converted by sampling into an audio frequency facsimile for filtering, amplification and recording. Data are recorded digitally for later processing, but can be simultaneously displayed or quickly played back in strip chart form.

### Control unit

The radar system used was manufactured by the GSSI company (Geophysical Survey Systems, Inc., North Salem, N.H.). The control unit was a SIR Model 4800 mainframe that triggers pulses at a repetition frequency of approximately 50 kHz and compiles the received pulses into 25.6 scans/s (higher or lower rates are possible). A variety of gain functions may be applied over the time range of the scans to suppress high amplitude early returns (especially the direct coupling between transmit and receive antennas) and enhance low amplitude later returns. The control unit also sets the time range of each scan, which can be varied from tens to thousands of nanoseconds.

### Antennas

A GSSI model 101C transducer unit was used in this study. The unit contains both transmitter and receiver electronics and the transmit and receive antennas, which are separated about 15 cm. The antennas are backshielded

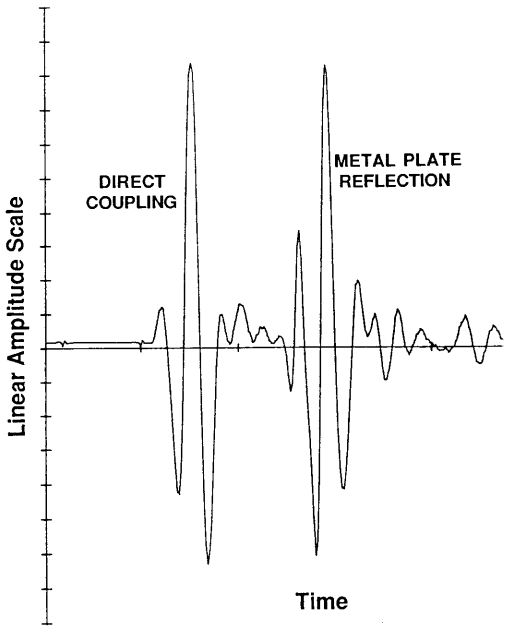


*Figure 1. Short-pulse waveform radiated in air by the GSSI Model 101C antenna. The center frequency is approximately the inverse of the period of the strongest oscillation.*

flared dipoles with a resistive end-loading to inhibit current oscillation. The waveform of a typical wavelet radiated in air by the model 101C is shown in Figure 1. The wavelet lasts about 3 ns and is commonly characterized by the frequency corresponding to the period of one oscillation—about 870 MHz for the 101C during the experiments conducted. The bandwidth is about 60% (higher bandwidths can be achieved with unshielded antennas, which can shorten the wavelet to almost an ideal doublet). Theoretical subsurface radiation patterns are multilobed (Engheta et al. 1982), but in air the pattern is dominated by a single broad lobe, whose 3-dB beamwidth is about 70° in both principal radiation planes (Arcone et al. 1986). For this study the antenna housing was fixed to a wooden plank and suspended over the sandbox by attaching the plank to the bucket of a tractor. The tractor then moved slowly along the sandbox to do the profiles.

### Data processing, display and interpretation

All data were recorded in scans of 512 eight-bit words on a GSSI DT6000 tape recorder, and then loaded and processed by the RADAN 3.0 (Boucher and Galinovsky 1989) program on a personal computer. Data can be displayed in either a wiggle trace (amplitude versus time of each scan) or line scan (intensity as color or shades of grey versus time) format as shown in Figure 2. Individual scans can be retrieved with the program. The only signal processing used was a horizontal high pass filter, which subtracts the average of many scans on either side of a particular scan from that particular scan. This filter effectively eliminated any signal that arrived at a constant time delay over the length of the filter, which is measured in number of scans. Thus, reflections from objects that increase in distance as the antenna moves (mainly the voids and end walls) improve in quality as unwanted clutter from the tractor, antenna supports, sandbox sidewalls, surface and bottom are suppressed. This filter was thus extremely useful in isolating the void reflection waveforms. Data interpretation is based mainly on the simple echo delay formula

$$d = ct/2n \quad (1)$$

where $d$ = depth of a reflector (centimeters)
$t$ = echo time delay (nanoseconds)
c = speed of electromagnetic waves in a vacuum (30 cm/ns)
$n$ = real part of the complex index of refraction of the medium through which the waves have propagated.

For a low loss medium such as dry sand, $n$ may be replaced by $\sqrt{\varepsilon}$ where $\varepsilon$ is the dielectric constant. The factor of two in eq 1 accounts for the round trip propagation path of the pulse. Equation 1 applies only to reflections emanating from horizontally flat interfaces of several in-situ wavelengths extent, or to scattering from point sources when the location of the point is known. Diffracted arrivals generated by inhomogeneities or sloping interfaces can be imaged properly by using the technique of diffraction migration. This will not be used here as the waveforms within the diffractions themselves are the subject of study.

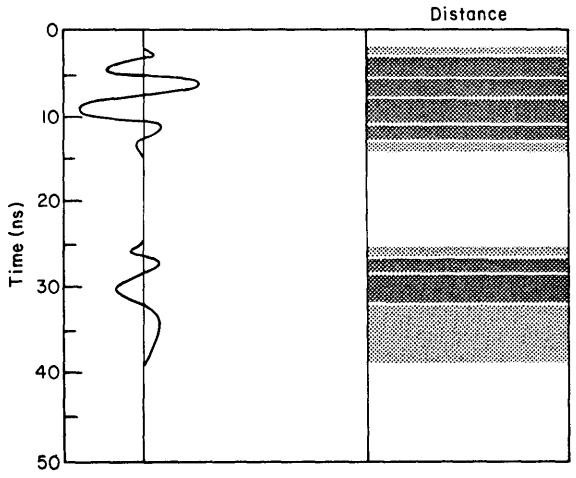


*Figure 2. Idealized wiggle trace scan display (right) and equivalent line scan intensity display should these returns remain constant with distance.*

## SCALE MODEL

The interaction of short-pulse radiation of characteristic in-situ wavelength $\lambda$ with square cross-sectional voids in bedrock of dimension $a$ is properly modeled so long as the ratio $a/\lambda$ is preserved, and the material conductivity is insignificant (e.g., Stratton 1941). The conductivity of a dry sand is generally less than 0.001 S/m, as it is also for ice or crystalline rock, which ensures that conductivity would not affect the wavelength at either the full scale or model frequency. Conductivity can also affect the scaling of a particular void depth if one is to preserve the ratio of input power to target distance for the particular system modeled—in this case about a 2.1-W peak (manufacturer's specification) to about a 70- to 120-cm target distance. However, in our modeled situation, the estimated skin depth is about five times greater than the void depths and so no appreciable effect of conductivity is expected upon the form or amplitude of the reflected pulses. Conductivity values greater than

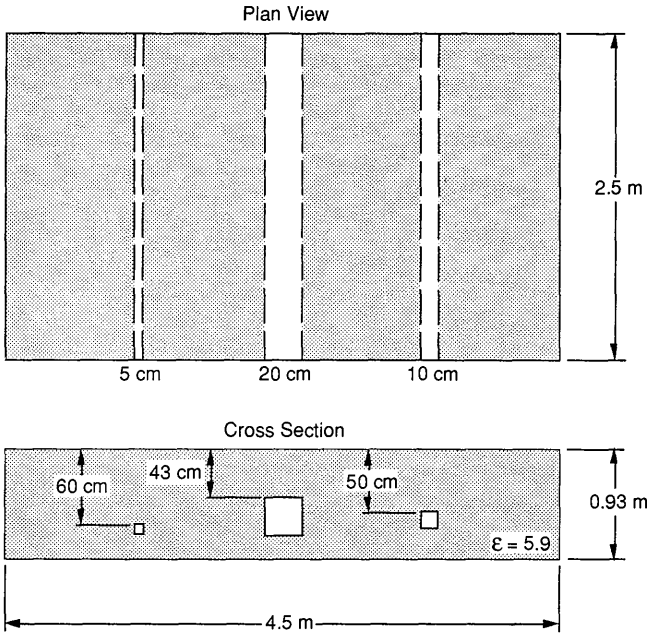


*Figure 3. Plan and front view of the sandbox model.*

about 0.01 would probably cause some pulse distortion in the modeling beyond that to be seen from the influence of the voids.

Figure 3 is a plan and front view of the sandbox model. The walls are constructed of 93-cm (3-ft) cubic blocks of concrete and the bottom is a reinforced concrete pad. Three square Styrofoam strips of 5-, 20- and 10-cm widths were placed across the box at depths of 60, 43 and 50 cm respectively. The strips were spaced 120 cm apart and were wrapped in polyethylene sheeting to keep out moisture. The free space wavelength at the pulse center frequency of 870 MHz in relation to the size of the voids gives full-scale frequencies of 22, 44 and 87 MHz for a 2-m size void.

The time delay between reflections returning from the sand surface and the concrete substrate gave an $\varepsilon = 5.9$ for the sand, which is in the range of most igneous rocks. Felsic granites have $\varepsilon$ values between 5.3 and 7.0 in the megahertz range, while mafic types tend to be slightly higher as do marbles and foliated metamorphic rocks (Keller 1984). Lower $\varepsilon$ values are found in quartzites (4.5) and ice (3.2). Dry sand has an $\varepsilon$ of about 2.6, so that this sand had a slight moisture content of about 2%. Whatever conductivity this caused, it was not sufficient to affect the pulse waveform, as will be seen later.

The antenna unit was fixed to a wooden plank, which, in turn, was attached to the hydraulically lifted dump on a tractor. The tractor then moved along the side of the sandbox to profile the voids. Altitude above the sand surface varied between about 23 and 85 cm during any one profile, and the two profiles to be discussed were made at slightly different average altitudes. These altitude limits correspond to about 0.7 and 2.2 wavelengths in the scale model and, therefore, about 10 to 30 m at 22 MHz and about 5 to 15 m at 44 MHz.

The center frequency of the pulse spectra gives a dominant wavelength within the sand of about 14 cm. This makes the ratios of void size to dominant in-situ wavelength about 0.35, 0.70 and 1.40 for the 5-, 10- and 20-cm voids, respectively, a ratio range that should give a strong response to either polarization. In addition, the simulated frequencies of 22, 44, and 87 MHz all have theoretical skin depths in highly resistive (greater than 10,000 Ωm) rock or ice in excess of 100 m, ensuring good penetration at these frequencies. Higher frequencies would give better void responses, but insufficient penetration.

The major limitations to this model are 1) the idealization of the surface as being flat, smooth and with no dielectric stratification, and 2) unwanted reflections (clutter) from the sides and bottom of the sandbox. Modeling granitic bedrock or ice as a low loss, homogeneous medium is valid as long as the bedrock is not badly weathered or fractured. At a modeled frequency of 22 MHz, the wavelength in air is about 14 m (7 m at 44 MHz). Consequently, at 22 MHz the maximum surface roughness should be no worse than about 1 m (about 0.3 m at 44 MHz) over the ground surface beam-intercept area, the diameter of which is about 7 m at a 5-m altitude and 14 m at a 10-m altitude. These are not severe restrictions for most terrain. More restrictive is the demand for surface dielectric homogeneity. Heavy vegetation, or several meters of soil overburden or deep weathering (i.e., decomposition and fracturing of the bedrock), can severely degrade a signal both through attenuation in propagating through the surface layers, and in reflections from these layers. Consequently, under these conditions the model would best simulate wintertime operation when unfrozen moisture and vegetation is minimal.

## RESULTS AND DISCUSSION

Figures 4a and b show two airborne profiles over the buried voids. Figure 4a is for the electric field polarized parallel to the void axes and Figure 4b for the perpendicular case. The records are in wiggle trace format, are cropped to 20- and 30-ns segments of the original record (Fig. 4a and 4b respectively), and are each about 300 scans long. The 0-ns reference is placed at the position of the antennas, with 0.5 ns added to account for the inter-antenna spacing. In each figure the upper profile is the raw data, the middle profile is the raw data with a

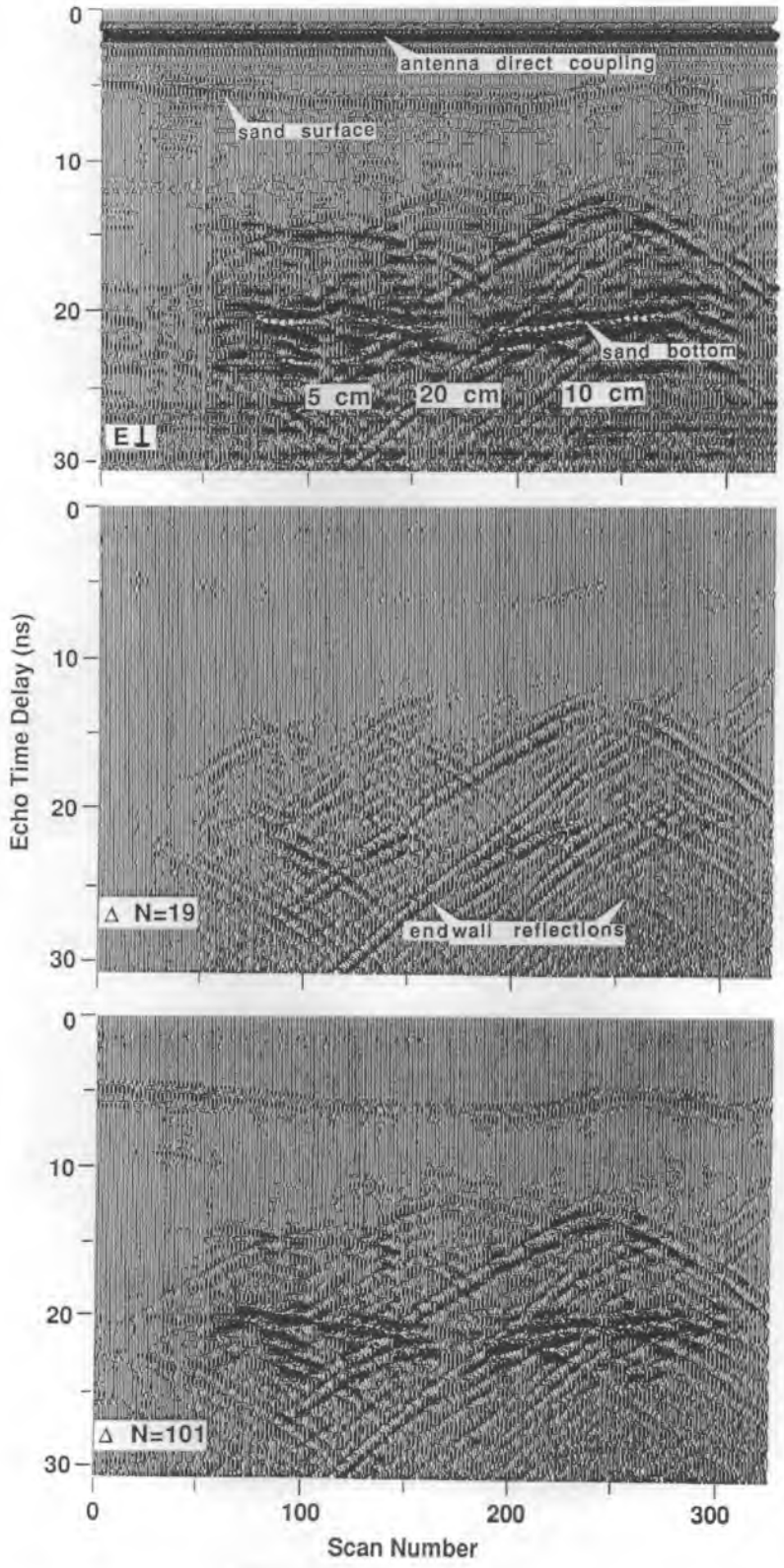


*b. Perpendicular polarization.*

*Figure 4 (cont' d). Wiggle trace format displays of the parallel and perpendicular polarization profiles.*

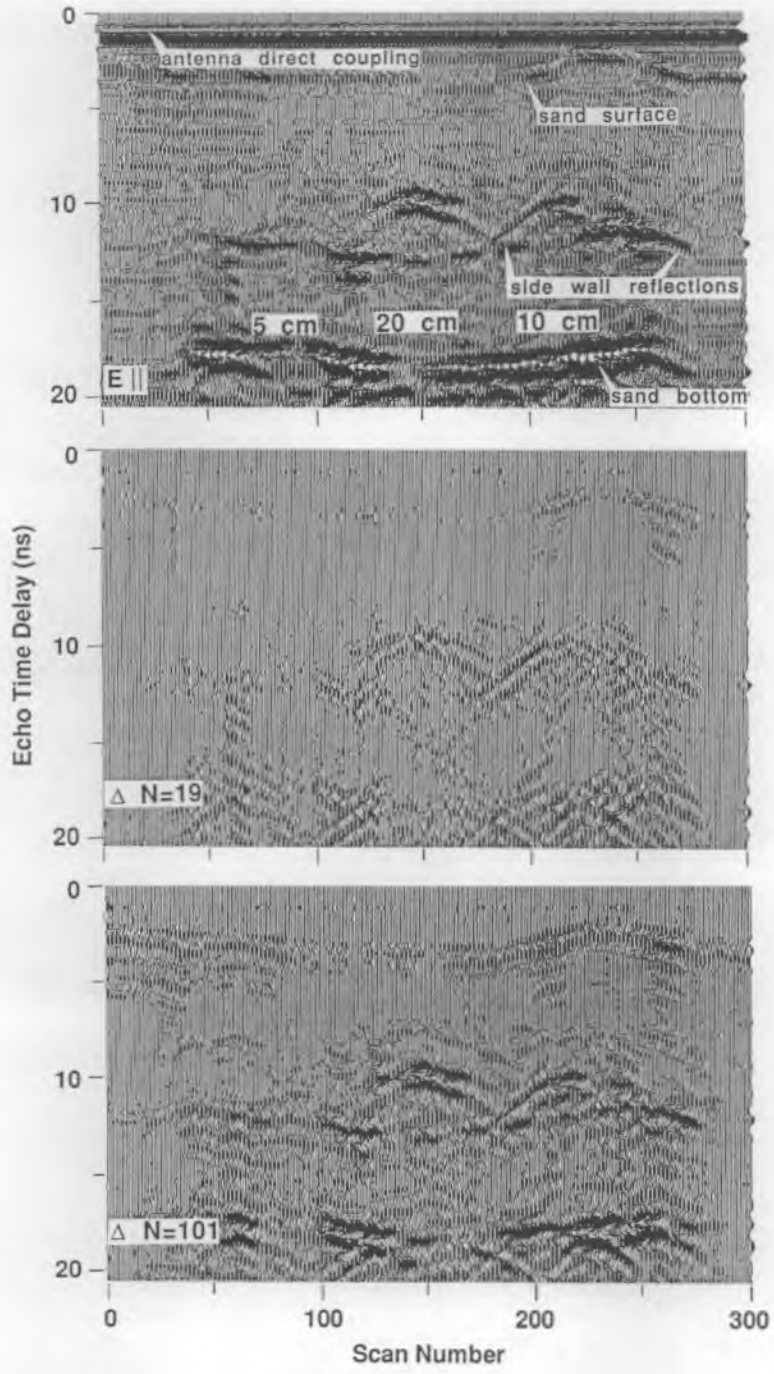


*a. Parallel polarization.*

*Figure 4. Wiggle trace format displays of the parallel and perpendicular polarization profiles.*

background removal filter applied that is 19 scans wide with a triangular weighting function, and the lower profile has the same filter, but is 101 scans wide. The triangular weighting emphasizes the scans nearest the center scan in computing average values along each scan. The uneven speed of the tractor prevents use of an exact linear horizontal distance scale, but the entire distance is 4.5 m. The same time range gain function was used for each profile.

In all profiles in Figure 4, the sand surface, which was level, appears to vary slightly in height because of antenna height changes. This event is followed by a series of three hyperbolas corresponding to each of the voids. Beneath the hyperbola peaks in both Figures 4a

and b are some bands starting at about 15 ns after the surface reflection. This is the sand/concrete pad interface at 0.93 m depth and the time delay gives an $\varepsilon = 5.9$. Just below the hyperbola peaks in Figure 4a are reflections identified as a side wall response because their time delays correspond to the round trip air distance to the sidewall edge. Running diagonally across the record in Figure 4b are several events identified as air waves reflected from the end walls; they are seen most clearly in the middle profile.

It is apparent that all three voids produce visible responses, with the weakest being for parallel polarization over the 5-cm void. The parallel polarization profile shows the strongest response to the 10- and 20-cm voids, about twice the amplitude at the peak of the hyperbola of the 5-cm void response (waveforms shown later). The perpendicular polarization profile shows the strongest response to the 10-cm void, but surprisingly, at positions slightly off axis on both sides of the hyperbola peak; for example, the amplitude at scan 259 is found to be about 50% higher than the amplitude of scan 240 at the hyperbola peak. The perpendicular response to the 5-cm void is nearly as strong at about 70% of the amplitude of scan 259. The 20-cm void response is the weakest at only about one-third of the strength of the 10-cm case. These 5- and 10-cm responses are manifested by prominent hyperbolas, some of whose asymptotes extend about 3 m both to the right of the 5-cm void and to the left of the 10-cm void on the perpendicular polarization record. It is apparent from the filtering that along the lengths of these hyperbolas there are at most four bands, corresponding to the two oscillations of the input waveform (Fig. 1). This implies that if there is any resonance to the reflections, it is not a major effect. This is borne out by examination of some of the filtered waveforms, shown later.

The airborne theoretical response for a point target 50 cm deep in sand ($\varepsilon = 5.9$) is shown in Figure 5. The response is not an exact hyperbola, as such shapes occur only for one-layer cases. The responses in Figure 5 are computed for antenna altitudes of 60 and 82.5 cm and are to be compared with the response 100 cm off-axis to the 10-cm void (about scan 175 in Fig. 4b), which shows a 4.5-ns increase in time delay from the peak response. Subtracting 1.0 ns for the altitude increase of 22.5 cm, the actual increase of 3.5 ns is what theory predicts. However, there is contamination of the hyperbolas from the walls and bottom. For example, the 10-cm void response crosses an end wall reflection around scan 254 for perpendicular polarization, and crosses a side wall response for parallel polarization around scan 245. There is also much overlap between hyperbolas and so most of the scans analyzed next are picked from the hyperbola peaks where this overlap is minimal.

Figure 6 shows several individual scans extracted from the filtered ($N = 101$) parallel and perpendicular polarization profiles respectively. Each sequence of three scans is taken near the peaks of the hyperbolas; the middle scan of each sequence is at the peak. Both the sand surface and the void responses are darkened; the darkened areas were chosen on the basis of the number of oscillations that consistently appear throughout the hyperbolas (e.g., Fig. 7). The periods of the void reflections are the same as those of the surface reflections and center all the pulse spectra between 850–900 MHz. In addition, all the void reflections are similar in waveform to that of the incident wavelet—for example, Figure 1 or

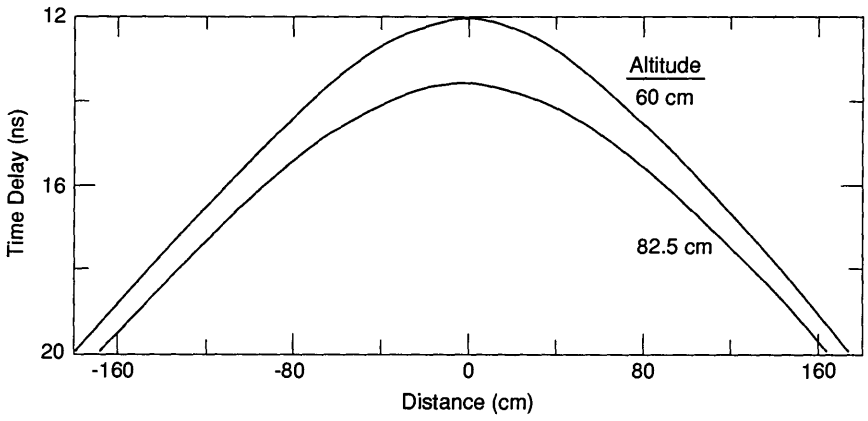


*Figure 5. Spatial distribution of radar wavelet time delays received at 60- and 82.5-cm altitude from a point scatterer located 50 cm deep in an $\varepsilon = 5.9$ dielectric medium. The time delays at different off-void axis distances are those seen in Figure 4b for the 10-cm void.*

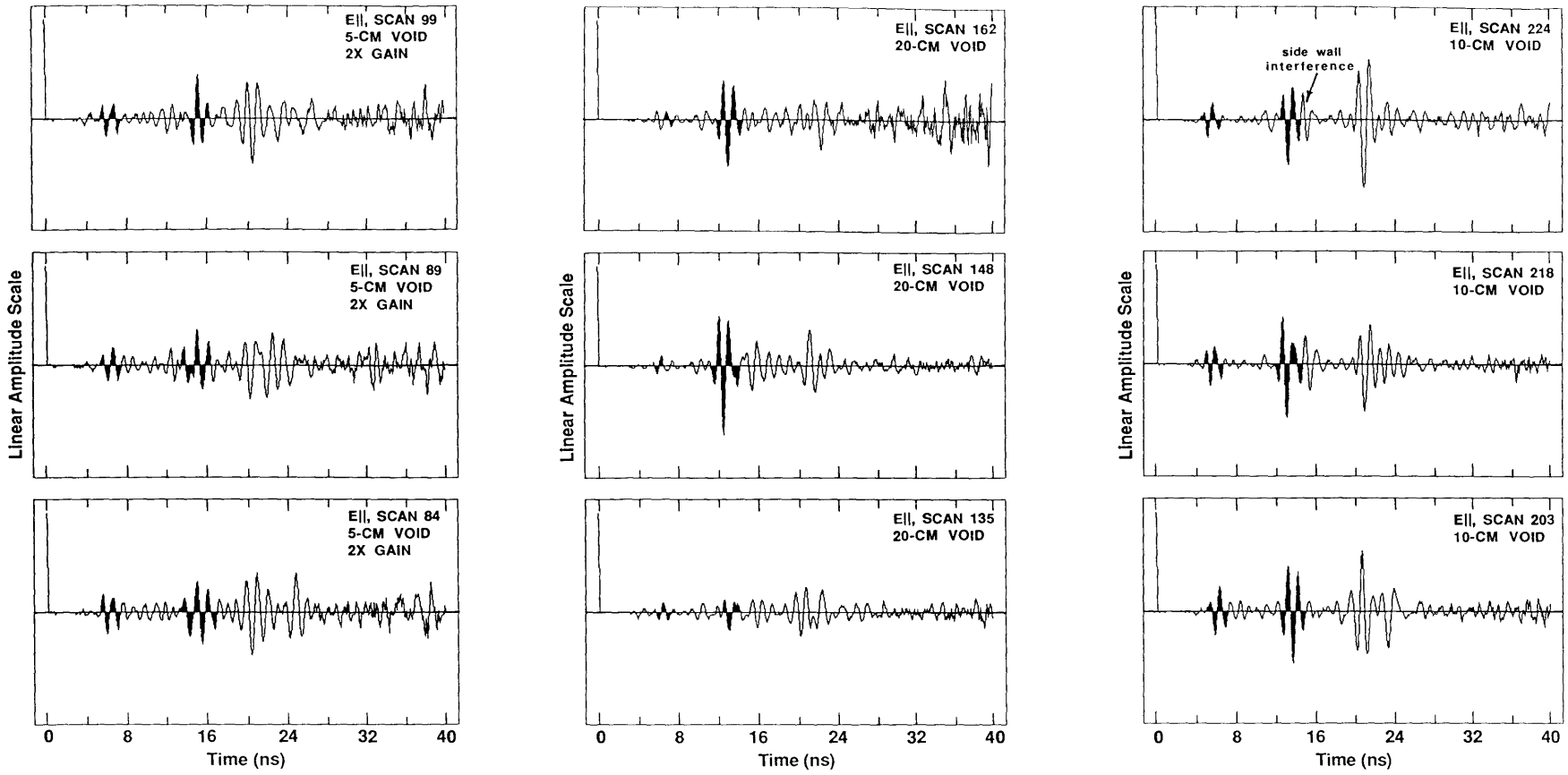


*a. Parallel polarization.*

*Figure 6. Individual scans extracted from the* N = *101 filtered profiles of Figure 4. The surface and void responses are darkened. The time range gain function is the same for all scans, but some scans have a constant gain factor of 2 to facilitate the display. The 0-ns reference begins at the trigger pulse that starts the scan rather than at the antenna position, which is the very first signal arrival.*

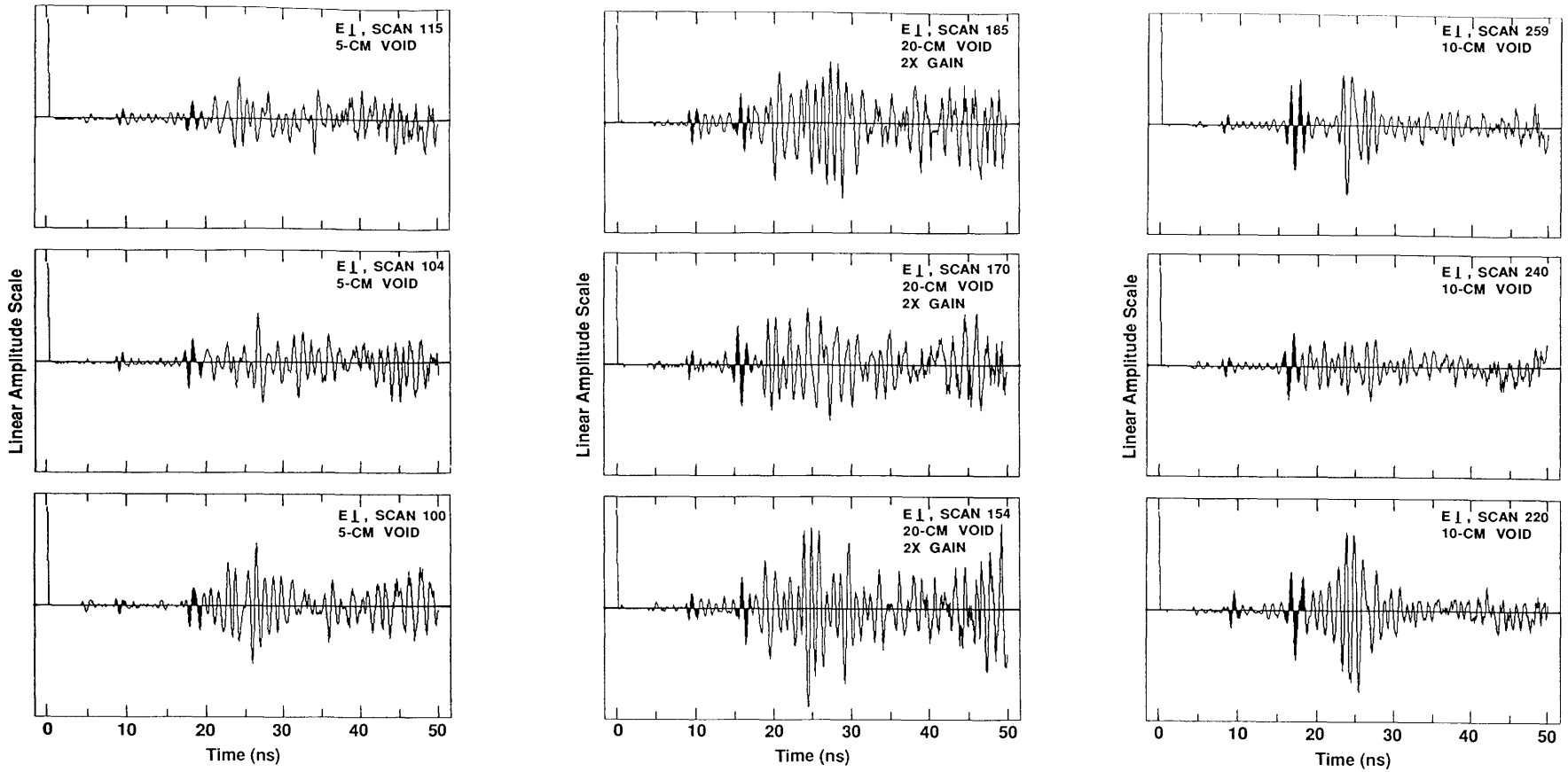


*b. Perpendicular polarization.*

*Figure 6 (cont'd).*

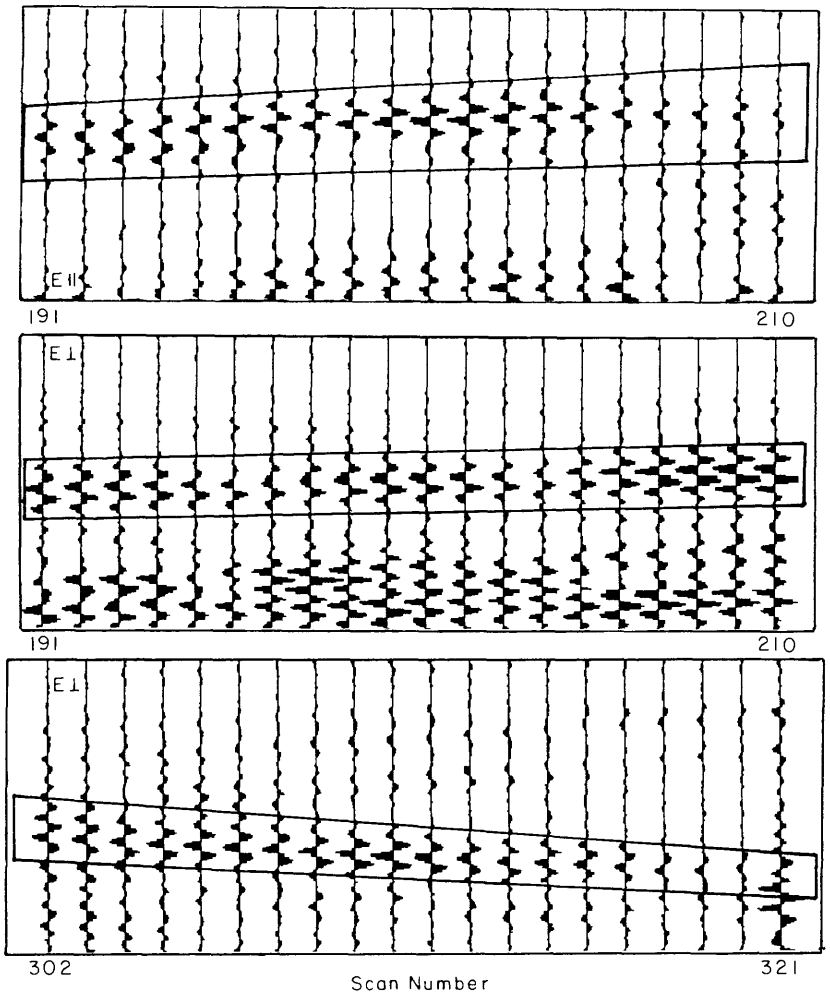


*Figure 7. Wiggle trace display of sections of 20 scans containing reflections from the 10-cm void for both parallel (top, scans 191–210) and perpendicular (middle, scans 191–210; bottom, scans 302–321) polarizations. Background removal filter is for* N = *19. The part of the responses that is consistent from trace to trace contains no more than four major half cycles, as does the input waveform of Figure 1.*

the surface reflection of scan 203 for parallel polarization. Scan 203 is also strong enough to show the polarization reversal between the sand surface and void reflections, as expected for opposing contrasts in dielectric constants between air and sand. It is therefore apparent that there is little, if any, resonance or peculiar character in the void reflections.

As discussed above, the strongest response for parallel polarization occurs for the 20-cm void and the weakest for the 5-cm void (note the 2× gain). For perpendicular polarization, the strongest response occurs for the 10-cm void and the weakest for the 20-cm void. The amplitudes of the surface reflections are not indicative of the amplitude strength incident upon the void; they are more affected by the filtering than are the void reflections. The time range gain function strongly accounts for maintaining amplitude along the hyperbolas near their peak, as in the case of the 10-cm void (perpendicular polarization), where the amplitude increase off axis is particularly strong. For example, the applied gain increases by a factor of 1.5 from the 20-ns delay at scan 240 (peak of the hyperbola), to the 24-ns delay off peak (scan 220), which strongly overcompensates for any decrease caused by further antenna distance.

Although there is no theory available for scattering from a square void in a dielectric matrix, the theory for infinite circular cylinders (Ruck et al. 1970) is thought to be very similar,* especially the case of a dielectric cylinder in air, which should have some similarities to

*Personal communication with R. Greenfield, Pennsylvania State University, 1990.

the present problem. Over the radius-(taken as half the void width)-to-in-situ-wavelength ratios of 0.18, 0.36 and 0.72 for the 5-, 10- and 20-cm voids, respectively, the backscattering cross section of a perfectly conducting cylinder varies insignificantly for parallel polarization, but for perpendicular can vary by approximately 3 dB about the parallel value. This variation is attributable to surface modes traveling around the cylinder. For a dielectric cylinder, however, exact solutions worked out for $\varepsilon = 2.56$ show an oscillatory behavior in the backscattered strength for both parallel (about a 6-dB range) and perpendicular polarization (the strongest backscattered strength is about 3 dB weaker than for the strongest parallel strength, but with very deep nulls) as a function of the radius-to-wavelength ratio. This increase in variability is ascribable to the extra phenomenon of internal oscillations. Internal oscillations and surface modes can easily be supported for this case of a square air cylinder in a dielectric medium, but they may be so severely damped as to only vary the strength of the backscattered signal and not to cause waveform changes.

## CONCLUSIONS

The results show that airborne detection of real, horizontal, rectangular voids of about 2-m dimension within a homogeneous dielectric can be obtained with short-pulse radar transmitting at center frequencies in the 20- to 90-MHz bandwidth and having its electric field polarized transverse to the void axis. Since present theory implies great variability in backscattered amplitudes, the dielectric constant of the host medium and the void dimensions should be known so that the appropriate pulse center frequency can be chosen to simulate the results found here. Pulse center frequencies in the 40- to 50-MHz range are recommended for a granitic medium for which the dielectric constant is about 5–7. If the host dielectric is a more mafic type of granite, such as gabbro for which $\varepsilon$ can be as high as 9, then the frequency must be lowered to preserve the same void-size-to-in-situ-wavelength ratio—to about 35 MHz for $\varepsilon = 9$. For a quartzite, the frequency would be about 50 MHz and for ice about 60 MHz. However, the wide bandwidth of a ground-penetrating radar short pulse implies that a center frequency of about 45 MHz should excite a strong response in all these cases. Under these conditions the reflected waveform is likely to be similar to that of the incident waveform over a variety of void sizes.

The peak power to depth ratio used here implies that only about 20 W would be needed to detect a void at a 12-m depth, either with polarization perpendicular or parallel to the void axis. The complicating factor is clutter from competing geologic targets, and attenuation from conductive absorption (as in a wet soil overburden) and scattering. The fact that perpendicular polarization worked well is advantageous for airborne work with linear antennas flying transversely across subsurface voids.

## LITERATURE CITED


**Annan, A.P. and J.L. Davis** (1976) Impulse radar sounding in permafrost. *Radio Science*, **11**(4): 383–394.

**Annan, A.P., J.L. Davis and D. Gendzwill** (1988) Radar sounding in potash mines. *Geophysics*, **53**(12): 1556–1564.

**Arcone, S.A.** (1988) Some airborne applications of subsurface radar. *Proceedings, Transportation Research Board 67th Annual Meeting, January 1988, Washington, D. C.*

**Arcone, S.A.** (1990) UHF model experiments of airborne short-pulse radar void detection in the HF band. Abstract presented at the *Third International Conference on Ground Penetrating Radar, 14–18 May, 1990, Lakewood, Colorado.*

**Arcone, S.A. and A.J. Delaney** (1987) Airborne river-ice thickness profiling with helicopter-borne UHF short-pulse radar. *Journal of Glaciology*, **33**(115): 330–340.

**Arcone, S.A., A.J. Delaney and R.E. Perham** (1986) Short-pulse radar investigations of freshwater ice sheets and brash ice. USA Cold Regions Research and Engineering Laboratory, CRREL Report 86-6.

**Boucher, R. and L. Galinovsky** (1989) *RADAN 3.0. Signal Processing Software.* Hudson, N.H.: Geophysical Survey Systems, Inc.

**Dallimore, S.R. and J.L. Davis** (1987) Ground probing radar investigations of massive ground ice and near surface geology in continuous permafrost. In *Current Research, Part A, Geological Survey of Canada*, Paper 87-1A, p. 913–918.

**Delaney, A.J., S.A. Arcone and E.F. Chacho, Jr.** (1990) Winter subsurface radar studies on the Tanana River. *Arctic*, **43**(3):244–250.

**Engheta, N., C.H. Pappas and C. Elachi** (1982) Radiation patterns of interfacial dipole antennas. *Radio Science*, **17**: 1557–1566.

**Greenfield, R.J.** (1988) Modeling of electromagnetic propagation between boreholes. In *Third Technical Symposium on Tunnel Detection Proceedings, 12–15 January 1988, Golden, Colorado.* Colorado School of Mines, p. 156–172.

**Jacobel, R.W. and S.K. Anderson** (1987) Interpretation of radio-echo returns from internal water bodies in Variegated Glacier, Alaska, U.S.A. *Journal of Glaciology*, **33**(115): 319-323.

**Jezek, K.C., C.R. Bentley and J.W. Clough** (1979) Electromagnetic sounding of bottom crevasses on the Ross Ice Shelf. *Journal of Glaciology*, **24**(90): 321–330.

**Keller, G.V.** (1984) Electrical properties of rocks and minerals. In: *CRC Handbook of Physical Properties of Rocks, Vol. I* (R. S. Carmichael, Ed.). Boca Raton, Florida: CRC Press.

**Kovacs, A. and R.M. Morey** (1985) Electromagnetic measurements of multi-year sea ice using impulse radar. USA Cold Regions Research and Engineering Laboratory, CRREL Report 85-13.

**Moffatt, D.L. and R.J. Puskar** (1976) A subsurface electromagnetic pulse radar. *Geophysics*, **41**(3): 506–518.

**Moran, M.L.** (1989) Time domain analysis of electromagnetic scattering for a three dimensional tunnel in the presence of a vertically oriented electric dipole. M. S. thesis, Pennsylvania State University (unpublished).

**Ruck, G.T., D.E. Barrick, W.D. Stuart and C.K. Kirchbaum** (1970) *Radar Cross Section Handbook*. New York: Plenum Press.

**Shih, S.F. and J.A. Doolittle** (1987) Using radar to investigate organic soil thickness in the Florida Everglades. *Soil Science Society of America Journal*, **48**(3): 651–656.

**Steinway, W.J., J.D. Echard and C.M Luke** (1981) Locating voids beneath pavement using pulsed electromagnetic waves. National Cooperative Highway Research Program Report 237. Washington, D.C.: Transportation Research Board, National Research Council.

**Stratton, J.A.** (1941) *Electromagnetic Theory*. New York: McGraw-Hill.

**Watts, R.D. and A.W. England** (1976) Radio-echo sounding of temperate glaciers: ice properties and sounder design criteria. *Journal of Glaciology*, **17**(75): 39–48.

**Watts, R.D. and D.L. Wright** (1981) Systems for measuring thickness of temperate and polar ice from the ground or from the air. *Journal of Glaciology*, **27**(97): 459–469.

# REPORT DOCUMENTATION PAGE

*Form Approved*
*OMB No. 0704-0188*



| 1. AGENCY USE ONLY (Leave blank) | 2. REPORT DATE | 3. REPORT TYPE AND DATES COVERED |
|---|---|---|
| | December 1990 | |

4. TITLE AND SUBTITLE

UHF Model Simulation of Detecting Voids in a Dielectric Medium Using HF-VHF Airborne Short-pulse Radar

5. FUNDING NUMBERS

RD&E Task No. A0H20010181

6. AUTHORS

Steven A. Arcone

7. PERFORMING ORGANIZATION NAME(S) AND ADDRESS(ES)

U.S. Army Cold Regions Research and Engineering Laboratory
72 Lyme Road
Hanover, New Hampshire 03755-1290

8. PERFORMING ORGANIZATION REPORT NUMBER

CRREL Report 90-11

9. SPONSORING/MONITORING AGENCY NAME(S) AND ADDRESS(ES)

U.S. Army Belvoir RD&E Center
Fort Belvoir, VA 22060

10. SPONSORING/MONITORING AGENCY REPORT NUMBER

11. SUPPLEMENTARY NOTES

12a. DISTRIBUTION/AVAILABILITY STATEMENT

Approved for public release; distribution is unlimited.

Available from NTIS, Springfield, Virginia 22161

12b. DISTRIBUTION CODE

13. ABSTRACT (*Maximum 200 words*)

A model study of the interaction between airborne-launched short-pulse radar signals and three sizes of rectangular voids in bedrock was conducted to see if polarization perpendicular to the strike of the voids could be used for detection, and if any characteristic waveform such as resonance could be associated with any of the void responses. Radar wavelets with frequency spectra centered at about 870 MHz illuminated three square Styrofoam (relative dielectric constant less than 1.1) strips, 5, 10 and 20 cm on a side, emplaced in a sand (relative dielectric constant of 5.9) box, 1 m deep, 4.5 m long and 2.5 m wide. This setup modeled the interaction of 22-, 44- and 87-MHz wavelets with voids having widths of 2 m and situated in a crystalline type of bedrock. The antennas traversed 23–85 cm above the sand surface and data were recorded continuously at 25.6 scans/s. Polarization both parallel and perpendicular to the long axis of the voids produced reflections with apparently undistorted wavelets and hyperbolic spatial distributions, with the strongest response for the perpendicular over the 10-cm void. Although real HF signal attenuation was not simulated in this model, the results suggest that under these nearly ideal conditions of a homogeneous void matrix of low conductivity with a flat surface, a 2-m void at a 10-m depth could be detected easily with a moderately powered transmitter at a 10- to 12-m altitude using a 40- to 50-MHz short pulse polarized perpendicular to the void axis.

14. SUBJECT TERMS

Cold regions; Dielectric targets; Ground penetrating radar; Ice; Soils; Void detection; Water supplies

15. NUMBER OF PAGES
19

16. PRICE CODE

| 17. SECURITY CLASSIFICATION OF REPORT | 18. SECURITY CLASSIFICATION OF THIS PAGE | 19. SECURITY CLASSIFICATION OF ABSTRACT | 20. LIMITATION OF ABSTRACT |
|---|---|---|---|
| UNCLASSIFIED | UNCLASSIFIED | UNCLASSIFIED | UL |

NSN 7540-01-280-5500

☆ U. S. GOVERNMENT PRINTING OFFICE: 1991--500-063--22056

Standard Form 298 (Rev. 2-89)
Prescribed by ANSI Std. Z39-18
298-102